17th Brazilian Congress of Thermal Sciences and Engineering
November 25th-28th, 2018, Águas de Lindóia, SP, Brazil

ENCIT-2018-0448
EXPERIMENTAL INVESTIGATION OF PRESSURE DROP IN ELECTRICAL SUBMERSIBLE PUMP (ESP) TURNED OFF UNDER LIQUID SINGLE-PHASE AND GAS-LIQUID TWO-PHASE FLOW

William Monte Verde
Cristhian Porcel Estrada
Jorge Luiz Biazussi
Antonio Carlos Bannwart
Valdir Estevam
University of Campinas, CEPETRO, R. Cora Coralina, 350 – Cidade Universitária, Campinas, SP, Brazil.
williammonteverde@gmail.com
cristhi8n@gmail.com
biazussi@unicamp.br
bannwart@fem.unicamp.br
valdir_e@hotmail.com

Paulo Sergio de Mello Vieira Rocha
Salvador José Alves Neto
Alexandre Tavares
psrocha@qgep.com.br
sneto@qgep.com.br
atavares@qgep.com.br
Queiroz Galvão Exploração e Produção S.A, Av. Almirante Barroso, 52, 1101 – Centro, Rio de Janeiro, RJ, Brazil.

Abstract.
The aim of this work is to experimentally determine the pressure drop in a ESP turned off. So, the main contribution of this study is to provide experimental correlations for local pressure drop that make it possible calculate the system curve and simulate an alternative production system. These results are essential for evaluating feasibility of the production layout studied. For this purpose, an experimental setup with the same ESP installed in the oil field was used to measure the pressure drop. The tests were carried out on oil single-phase flow at different flow rates and viscosities. In addition, gas-liquid two-phase flow tests were performed to investigate the gas influence on the pressure drop. The oil single-phase tests indicated the power law dependence between the loss coefficient and the Reynolds number. Based on these correlations, an estimative of the oil field pressure drop was performed. This study indicates a high pressure drop for the design conditions, requiring a careful evaluation of the production layout. The gas-liquid two-phase flow tests are in progress and will be presented in the final paper.

Keywords: *Electrical Submersible Pump (ESP), pressure drop, ultra-heavy oil, gas-liquid two-phase flow.*

1. INTRODUCTION

In recent years, large offshore reserves of unconventional oil have been discovered on the Brazilian coast and the perspectives are positive that these reserves continue to increase in a near future. The promising scenario of oil industry has motivated several national and international companies to invest in Brazil. However, the offshore operations are expensive at any stage of upstream chain, so the oil companies and the supply industry have worked hard to improve profitability by operating more efficiently and reducing costs, making new projects feasible even for low oil prices.

Several actions have been implemented to reduce operating costs, risks and uncertainty in the production of ultra-viscous oil. Some of these are related to the artificial lift system design. One of the few artificial lift methods available for offshore ultra-viscous oil production is the Electrical Submersible Pump (ESP). Flatern (2015) estimate between 150.000 and 200.000 wells producing oil using ESPs.

A conventional ESP consists of centrifugal pump stages mounted in series and driven by an electric motor placed on the producing well bottom. In addition, the system is composed of both downhole and surface equipment in offshore platforms. The production bottom hole assembly are designed based on the desired flow rate, required power, well conditions and geometry. The assembly is connected to surface controls and electric power. The ESP system has operational advantages over other artificial lift methods and its differential is the high production capacity. Furthermore, the ESP can operate in vertical, horizontal or deviated wells, in onshore or offshore applications (Takács, 2009).

The usual assembly, with the pump submersed at the production well bottom, has as main advantages flow assurance requirements, since the temperature and pressure in the pump intake are the highest possible. Thus, the oil viscosity and the Gas-Oil Ratio (GOR) are lower and the pump operates more efficiently. However, the workover costs of ESP positioned at the well bottom are extremely high. When the pump or any system component fails, it is necessary to interrupt the production, remove the ESP system and replace it with a new one. For wet completion wells, a dedicated workover rig is required. Usually, this rig is rented at a high cost and has limited availability in the supply chain.

The motivation of this work is related to the analysis of an alternative production layout using ESPs system, shown in Fig. 1, in order to increase the production profitability. This layout provides the installation of two multi-stage centrifugal pumps associated in series. The first one is installed conventionally at the well bottom hole, while the second pump is positioned on the seabed in a skid, called Subsea ESP Skid (S-ESPS). The S-ESPS is a recent technology and was primarily presented by Costa *et al*. 2013.

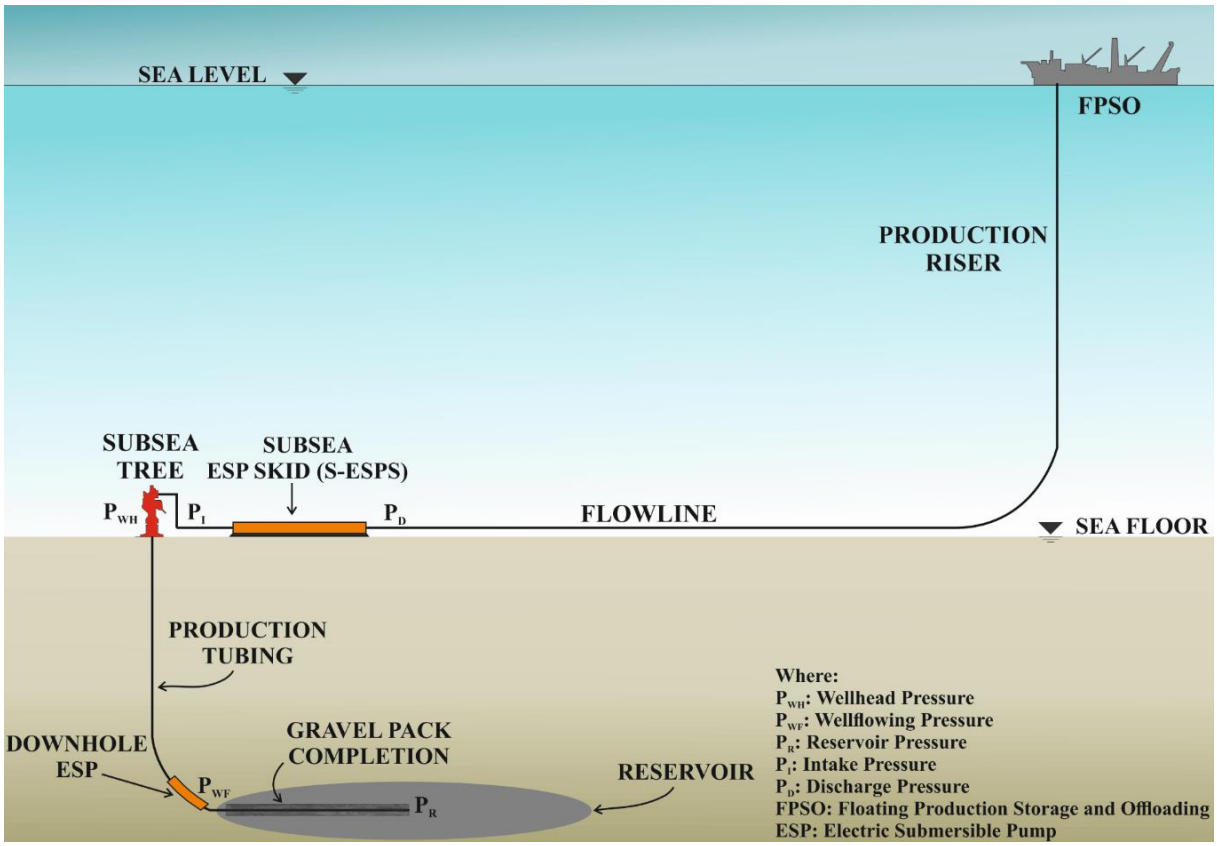

Figure 1. Layout of subsea production system.

The production system is carried out initially by the downhole ESP until its failure occurs, at which time the S-ESPS is put into operation. The advantage of this layout is not interrupt the production while the workover rig is coming and the S-ESPS can operate as backup until the well intervention. Since the two systems are assembled in series, the oil will have to flow through the downhole ESP turned off until it reaches the S-ESPS. Of course, the downhole ESP turned off will offer resistance to the fluid flow, which results in pressure loss. The local pressure loss changes the system curve resulting in a decrease in the produced oil flowrate. In addition, the ESP pressure drop can increase the GOR at the S-ESPS intake, impairing its performance. Therefore, it is evident the need to estimate the downhole ESP pressure loss depending on the operating conditions. Other researchers such as Jeong and Shah (2004), Mendes *et al.* (2007) and Calçada *et al.* (2012) have studied the pressure drop in fittings used in oil industry, however studies on the pressure loss in an ESP turned off are not reported in the literature.

The aim of this work is to experimentally determine the pressure drop in an ESP turned off. Therefore, the main contribution of this study is to provide experimental correlations for local pressure drop that make it possible calculate the system curve and simulate the production system. These results are essential for evaluating feasibility of the production layout studied. For this purpose, an experimental setup with the same ESP installed in the oil field was used to measure the pressure drop. The tests were carried out on oil single-phase flow at different flow rates and viscosities. In addition, gas-liquid two-phase flow tests were performed to investigate the gas influence on the pressure drop.

2. METHODOLOGY

This study was conducted in the Experimental Laboratory of Petroleum – LabPetro at UNICAMP. The experimental facility was especially design to measure ESP performance with ultra-heavy oil. However, in this case the facility was used to investigate the pressure drop that occurs when the fluid flow through an ESP turned off, either for liquid single-phase or gas-liquid two-phase flow.

2.1 Experimental facility

The ESP loop test is shown schematically in Fig. 2. The facility is composed basically of an oil tank, a two-screw booster pump, a temperature control system, an ESP, Variable Speed Drives (VSDs), valves, measure instrumentations, and a power generator. The booster, with nominal flow rate of 200 m³/h and head of 25 bar, pumps the oil from the tank through the pipes up to the ESP intake. This pump is driven by a VSD, allowing rotational speed control. Because it is a closed loop, the oil tends to heat up during the tests. So, a temperature control system, composed of a thermo-chiller and a heat exchanger with capacity of 230000 kCal/h, is used to keep the fluid temperature constant. This issue is fundamental, because the oil viscosity is controlled by its temperature.

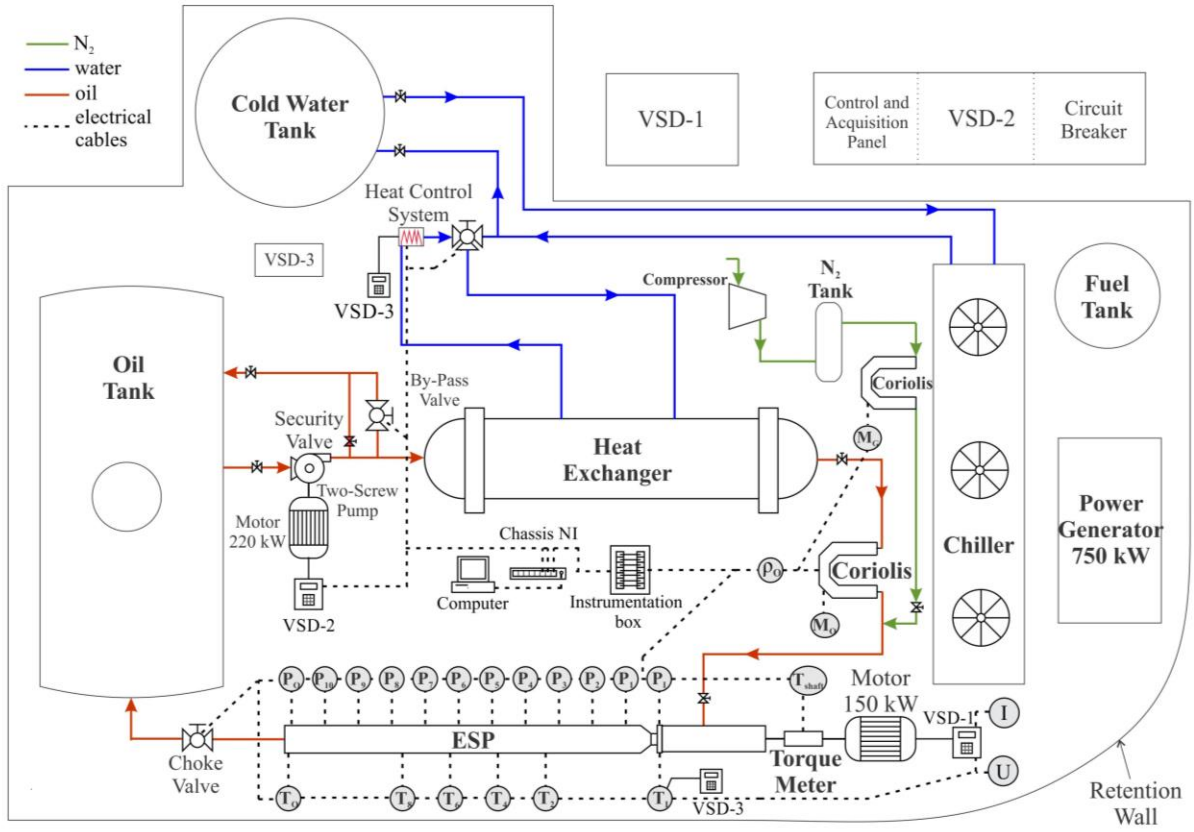

Figure 2. Schematic diagram of the ESP loop test.

.

2.2 Single-Phase Modeling

The pressure drop through the ESP turned off can be obtained by a control volume analysis. Considering liquid single-phase flow, steady-state, incompressible and isothermal flow between sections 1 and 2, as shown in Fig. 3, the integral energy equation becomes:

$$\left(\frac{P}{\rho_L g}+\varphi\frac{V_L^{\,2}}{2g}+z\right)_1-\left(\frac{P}{\rho_L g}+\varphi\frac{V_L^{\,2}}{2g}+z\right)_2=H_L \tag{1}$$

Where P is the pressure, ρ_L is the liquid density, g is the acceleration of gravity, φ is the correction factor of the kinetic energy, V_L is the liquid velocity, z is the elevation and H_L is the head loss.

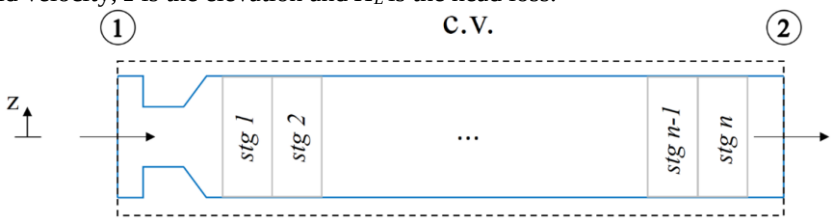

Figure 3. Control Volume for the ESP.

Neglecting the kinetic and gravitational terms, Eq. (1) is written as:

$$\frac{P_1 - P_2}{\rho_L g} = H_P \tag{2}$$

The term H_P refers to the local head loss. According White (1997), the flow pattern through a device is quite complex and the theory is very weak. The local losses are commonly measured experimentally and correlated with the flow parameters in tubes. The measured local loss is usually given as a ratio of the head loss through the device to the velocity head, so the loss coefficient (K) is:

$$K = \frac{H_P}{\frac{V^2}{2g}} = \frac{\Delta P_L}{\frac{1}{2}\rho_L V_L^{\,2}} \tag{3}$$

For the ESP turned off we can calculate a loss coefficient by measuring the pressure drop (ΔP_L) and the flow rate in order to calculate the reference velocity (V). Usually, the local head loss coefficient is correlated with the Reynolds number, defined by:

$$Re_L = \frac{\rho_L V_L D}{\mu_L} \tag{4}$$

Where D is the characteristic length, considered to be the outer impeller diameter and μ_L is the liquid dynamic viscosity.

According Coffield *et al*. (1997), the correlations adjusted for K can be written as:

$$K = C_1\, Re_L^{-C_2} \tag{5}$$

Where C_1 and C_2 are constants of the experimental fitting. After the correlation fitting between the loss coefficient and the Reynolds number, it is possible to estimate the pressure drop in the oil field scenario. The pressure drop due to the ESP turned off is:

$$\Delta P_L = \rho_L \sum K \frac{V_L^2}{2} \tag{6}$$

Substituting Eq. (5) into Eq. (6) and the coefficients sum by the stage number (N) of the ESP, the pressure drop is:

$$\Delta P_L = N\left(C_1\, Re_L^{-C_2}\right)\frac{\rho_L V_L^2}{2} \tag{7}$$

Rewriting the pressure drop based on parameters measured in the oil field:

$$\Delta P_L = \frac{NC_1}{2}\rho_L^{(1-C_2)}\left(\frac{Q_L}{A}\right)^{(2-C_2)} D^{-C_2}\mu_L^{C_2}$$

Where C_1 and C_2 are constants of the experimental fit. Thus, given the constants, it is possible to estimate the pressure drop knowing the fluid properties, the characteristic diameter and the flow rate.

2.3 Non-Isothermal Single-Phase Flow Modeling

In order to estimate the pressure drop through the ESP turned off, we can also consider the hypothesis of non-isothermal flow. In this case, it is assumed that all the energy dissipated as head loss is converted into heat. The heat generation heats the fluid and there is no dissipation to the external environment, thereby, the adiabatic flow hypothesis is considered. Thus, when flowing through each stage of the pump, the fluid undergoes a decrease in pressure and, consequently, an increase in temperature, as shown in Fig. 4.

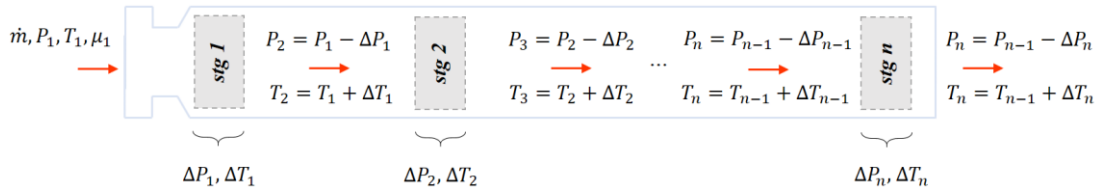

Figure 4. Temperature rise through the pump stages due to the heat dissipated in the pressure drop.

For a simplified approach, it is assumed that the power dissipated ($\dot{q}$), due to the head loss, is given by:

$$\dot{q} = \Delta P Q \tag{9}$$

Where ΔP is the pressure drop in the stage and Q is the volumetric flow rate.

As the flow is considered non-isothermal and adiabatic, all dissipated power is converted to heating the fluid. Therefore, the temperature increment is:

$$\Delta T = \frac{\dot{q}}{\dot{m} c_p} \tag{10}$$

Where c_p is the specific heat.

The procedure consists of calculating the head loss in the first stage and then the temperature increase. So, it is possible to correct the fluid viscosity at the output of the first stage and calculate a new Reynolds number. Then, the head loss at the second stage it is calculated, the temperature increase, the viscosity is corrected and the Reynolds number is recalculated. This procedure is repeated continuously until the last stage of the pump. Calculating the sum of the head loss of each stage is obtained the total ESP pressure loss.

2.4 Two-Phase Modeling – Homogeneous No-Slip Model

When the pressure is lower than the oil saturation pressure, the lighter fractions of hydrocarbons evaporate and gas-liquid two-phase flow occurs. Generally, the rigorous solutions of the conservations equations for the gas-liquid two-phase are complex and not available. A feasible approach for two-phase flow is to consider earlier models, which treat the system as single-phase flow. The Homogeneous No-Slip approach is an earlier model that treat the two-phase mixture as a pseudo single-phase fluid with average and fluid properties. The mixture fluid properties are determined from the single-phase gas and liquid properties, which are averaged on the basis of no-slip liquid holdup (Shoham, 2006).

Assuming steady-state one-dimensional flow, no slippage between the phases and that the phases are well mixed and in equilibrium, the average velocity and the average fluid properties can be calculated. The mixture average velocity (V_M) is given by:

$$V_M = \frac{Q_L + Q_G}{A} \tag{9}$$

Where Q_G is the gas volumetric flow rate.

The mixture density (ρ_M) is calculated as a weighting between phases properties:

$$\rho_M = \alpha \rho_G + (1 - \alpha) \rho_L \tag{10}$$

Where ρ_G is the gas density and α is the no-slip gas void fraction given by:

$$\alpha = \frac{Q_G}{Q_G + Q_L} \tag{11}$$

The mixture dynamic viscosity (μ_M) can be calculated by the model proposed by Dukler et al. (1964):

$$\mu_M = \alpha\mu_G + (1-\alpha)\mu_L \tag{12}$$

Where μ_G is the gas dynamic viscosity.

The pressure drop in the ESP turned off under gas-liquid two-phase flow, assuming homogeneous no-slip model, is calculated by Eq. 8. Therefore, average mixture properties must be considered and the constants C_1 and C_2 are the same fitted for the single-phase flow as:

$$\Delta P_{GL} = \frac{NC_1}{2}\rho_M{}^{(1-C_2)}\left(\frac{Q_M}{A}\right)^{(2-C_2)} D^{-C_2}\mu_M^{C_2} \tag{13}$$

Where ΔP_{GL} is the gas-liquid pressure drop.

In general, the accuracy of the homogeneous model is limited to the flow of small bubbles dispersed in a continuous liquid phase, which occurs commonly in mixtures with high liquid flow rates. In this study, the application range of the homogeneous model for pressure drop calculation is experimentally determined.

2.5 Experimental Procedure

To estimate the pressure drop through the ESP turned off it is necessary to carry out experimental measurements to calculate the loss coefficient and evaluate the parameter dependence with operating conditions, such as flow rate and viscosity. For this purpose, a representative experimental matrix was performed for the oil field conditions.

The experimental procedure consists in using the booster pump to provide a certain flow rate in the experimental loop, while the pressure drop across the ESP turned-off is measured. During the tests, the temperature is measured and the viscosity is controlled.

When there is flow through the ESP turned-off, there may be rotation induction in the equipment. Thus, the tests were performed in two configurations. In the first one, the ESP shaft was left free, being possible the induction of rotation by the oil flow. In the second configuration, the pump shaft was locked, making it impossible to rotate. This condition aims to represent a possible failure in the field where the shaft is locked, making the estimate of head loss more realistic.

The single-phase experimental matrix covers oil flow rates between 3.2 and 18.0 kg/s, viscosities of 0.130 to 1.600 Pa.s.

3. RESULTS

In this section, the results for tests with single-phase oil flow are presented. Tests with gas-liquid two-phase flow are currently underway and will be presented in the final full paper.

3.1 Liquid Single-Phase Flow

From the single-phase results measured in the tests with the free and locked shaft it is possible to calculate the loss coefficient using Eq. (3). For this, it is necessary to calculate the flow velocity. Due to the variations of area that occur inside the diffuser and pump impeller, the characteristic length will be considered the outer diameter of the rotor $D = 0.134m$. For the experimental results to be valid for the oil field application, it is necessary to base the analyzes on dimensionless numbers. Therefore, the loss coefficient is presented by stage and correlated with the Reynolds number.

Figure 4 and Fig. 5 present the experimental results for the loss coefficients per stage as a function of the Reynolds number in the free and locked shaft tests, respectively. In these figures, the fitted correlations between the loss coefficient and the Reynolds number are also presented.

By analyzing Fig. 5 and Fig. 6 it is possible to verify the power law ratio between the loss coefficient and the Reynolds number. The loss coefficient increases with decreasing Reynolds number. As the turbulence increases, the loss coefficient decreases with an asymptotic behavior and tends to be constant and independent of the Reynolds number. The fitted correlation for the free shaft test has a determination coefficient of $R^2 = 0.987$. This value represents a fitting measure of a generalized statistical model in relation to the measured values. The determination coefficient ranges from 0 and 1,

indicating in percentage how much the model can adjust the measured data. The greater the coefficient, more representative the adjusted correlation becomes. In the locked shaft test, the power law fitted presents determination coefficient of $R^2 = 0.935$.

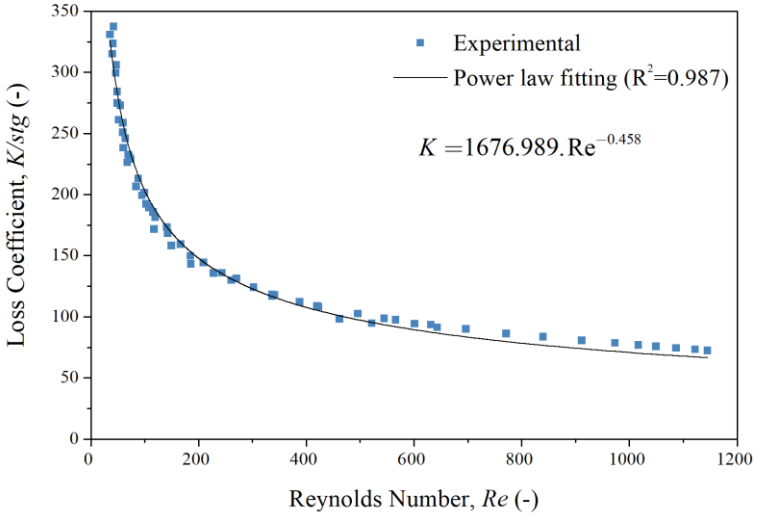

Figure 5. Loss coefficient per stage for the free shaft test.

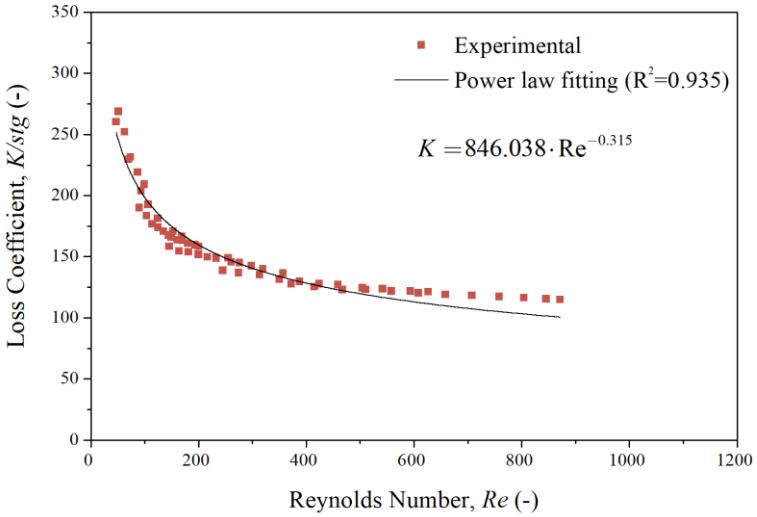

Figure 1. Local head loss coefficient per stage for the locked shaft test.

Figure 7 shows the comparison between the loss coefficients for the free and locked shaft tests. For Reynolds number less than 200 it is possible to observe that the loss coefficients are similar for the two test configurations. This result is expected since even as a free shaft, the low drag force is insufficient to induce rotation resulting in equal test configurations.

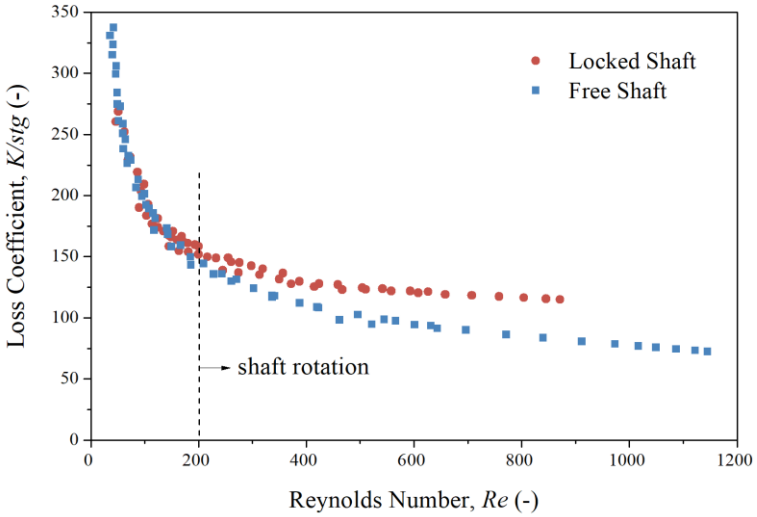

Figure 2. Comparison between the local head loss coefficients for the free and locked shaft.

However, for $Re > 200$ the pump shaft has induced rotation and begins to rotate due to the oil flow. Thus, the free shaft loss coefficient decreases compared to the locked shaft test. The lower loss coefficient when there is rotation induction is a physically coherent result because the fluid always flows in order to minimize energy loss. That is, inducing the rotation dissipates less energy than it does with the stopped rotors. In the tests with the free rotor an induced rotation up to 600 rpm was observed for high Reynolds numbers.

The pressure drop based on the fitted correlations was calculated by Eq. (3). The comparison between the pressure drop measured experimentally considering free shaft and that calculated by the correlation is shown in Fig. 8. In Fig. 9 the same comparison is made, however for the locked shaft setup. Analyzing these figures, it is observed that the fitted correlation provides good agreement with deviation range of +/-10%.

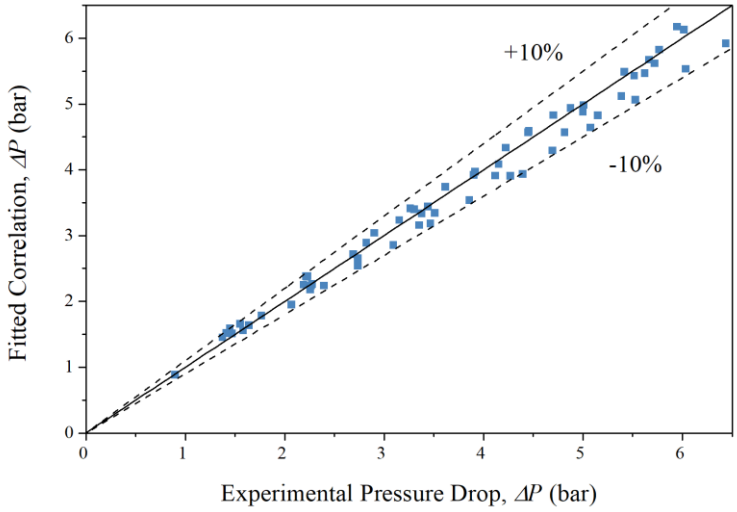

Figure 8. Comparison between the pressure drop obtained by the fitted correlation and the experimentally measured in the free shaft test.

3.2 Oil Field Simulation – Isothermal Single-Phase Oil Flow

Based on the fitted correlation of loss coefficients, it is possible to estimate the pressure drop on the oil field application. For the free shaft setup, the fitted constants are $C_1 = 1676.989$ and $C_2 = 0.458$. Assuming the outer impeller diameter of $D = 0.134m$, the pressure drop through an ESP turned off with free shaft is calculated by the Eq. (8), so:

$$\Delta P = 1503226.113 N \rho^{0,542} Q^{1.542} \mu^{0,458} \tag{11}$$

Where $\Delta P = Pa$, $\rho = kg/m^3$, $Q = m^3/s$, $\mu = Pa.s$ and N is the ESP stage number.

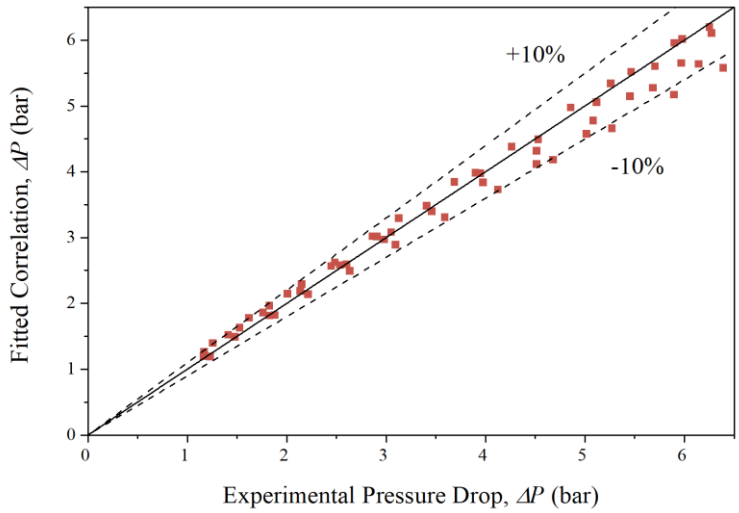

Figure 9. Comparison between the pressure drop obtained by the fitted correlation and the experimentally measured in the locked shaft test.

Similarly, for locked shaft setup the fitted constants are $C_1 = 846.038$ and $C_2 = 0.315$, and the pressure drop is calculated by Eq. (12):

$$\Delta P = 1046483.512 N \rho^{0,685} Q^{1.685} \mu^{0,315} \tag{12}$$

The ESP that will be considered in the oil field, according to Fig. 1, has about 100 stages. Assuming the oil density $\rho = 930 kg/m^3$, the estimated pressure drop through the ESP, with free shaft failure, as a function of oil viscosity and flow rate is shown in Figure 10. The estimated pressure drop for a locked shaft failure is shown in Figure 11.

The projected production flow rate for this field is approximately 65 m^3/h with oil viscosity of 400 cP. Under these conditions, for a free shaft failure, the analysis of Figure 10 provides pressure drop of approximately 82 bar. If the failure locks the ESP shaft at the same flow conditions, the pressure drop indicates about 96 bar (Figure 11). In both failure possibilities, the estimated pressure drop is high and can make the production layout unfeasible.

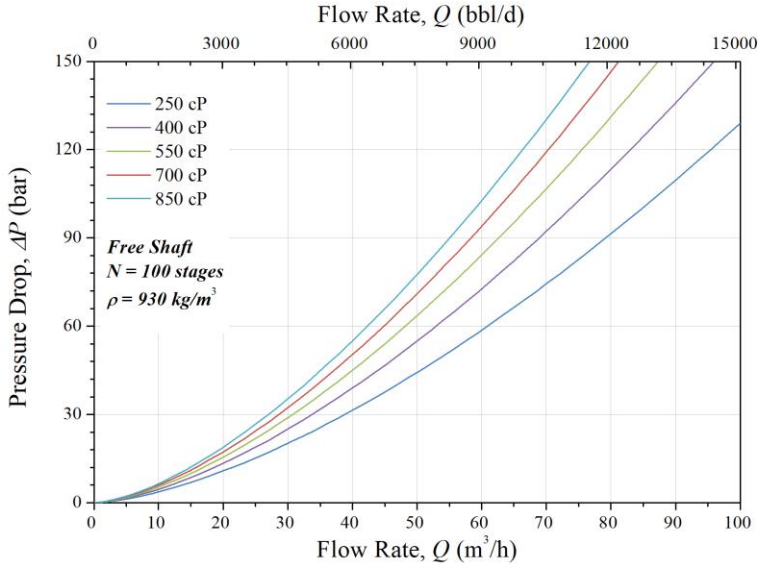

Figure 10. Pressure drop estimate of 100 stages ESP turned off with free shaft.

Figure 10 and 11 are useful for an initial analysis of the production system. Due to the well-reservoir coupling, it is necessary to simulate the entire production system considering the pressure drop predicted by the correlations presented in Eqs (11) and (12).

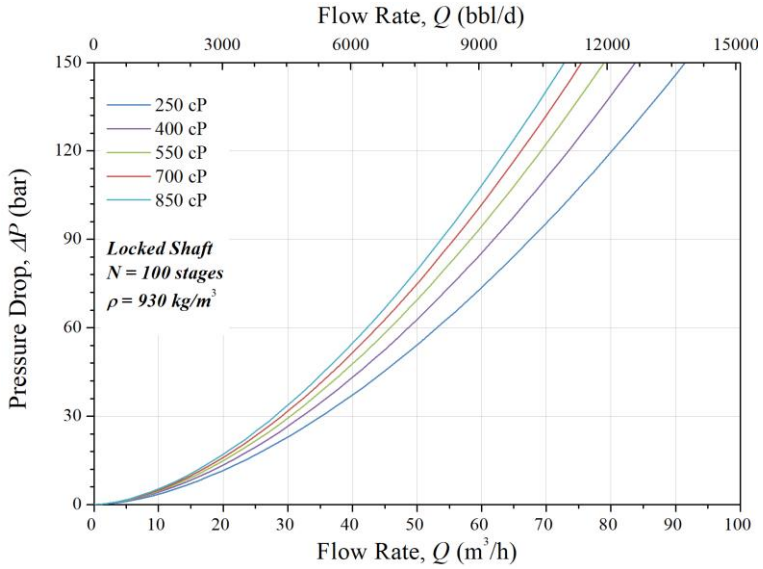

Figure 11. Pressure drop estimate of 100 stages ESP turned off with locked shaft.

3.3 Oil Field Simulation – Non-Isothermal Single-Phase Oil Flow

A second approach considers that the energy dissipated due to head loss heats the oil. In this way, the oil viscosity continuously reduces along the flow through the ESP, decreasing the pressure drop. Therefore, the non-isothermal approach provides lower pressure drop than the isothermal flow. In Figure 12 is shown the calculated pressure drop for non-isothermal flow for viscosities of 250 and 400 cP and a free shaft failure.

For the flow rate of 65 m^3/h and oil viscosity of 400 cP, Figure 12 indicates a pressure drop reducing of 6 bar. Considering as reference the isothermal flow, this difference represents a reduction of 7% in the pressure drop.

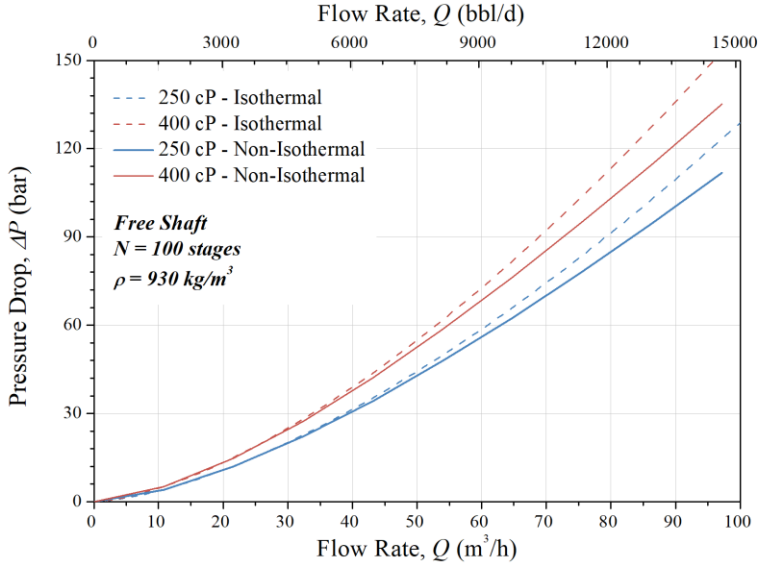

Figure 12. Isothermal and non-isothermal comparison.

3.4 Gas-Liquid Two-Phase Flow

The gas-liquid two-phase flow are under development and will be presented in full paper version.

4. CONCLUSIONS

In this study an experimental analysis of the pressure drop through an ESP turned off under liquid single phase and gas-liquid two-phase flow was performed. As preliminary results are presented the measured data of the oil single-phase flow tests. Based on these results, empirical correlations between loss coefficient and Reynolds number were fitted. The fitted correlations show a power law dependence between the loss coefficient and the Reynolds number. These correlations allowed to estimate the pressure drop in an oil field conditions for two failure possibilities, free and locked shaft. This study is relevant because it provides important data to numerically simulate the productions system and to assist in the design of the production system.

For the final paper, the present study will be extended to gas-liquid two-phase flow. The main objective is to adjust empirical correlations that can be used in field applications.

5. ACKNOWLEDGEMENTS

This study was supported by Queiroz-Galvão Exploração e Produção (QGEP) and National Agency of Petroleum, Natural Gas and Biofuels, Brazil, associated with investment funds from the R&D clauses. Acknowledgments are also extended to ALFA Research Group and CEPETRO/UNICAMP.

6. REFERENCES

Coffield, R. D, McKeown, P. T, and Hammond, R. B, “Irrecoverable pressure loss coefficeints for Two Elbows in Series with Varios Orientation and Separation Distances”, Bettis Atomic Power Laboratory, West Mifflin, PA, 1997.

Costa, B. M. P.; Oliveira, P. D. S.; Roberto, M. A. R. “Mudline ESP: Electrical Submersible Pump Installed in a Subsea Skid”. Offshore Technology Conference, p. 1–10, 2013. https://doi.org/10.4043/24201-MS

Flatern, R. V. “The Defining Series – Electrical Submersible Pumps”, Oilfield Review, 2015.

Takács, G., 2009, “Electrical Submersible Pump Manual”, 1. Ed., Elsevier, Oxford, UK, 2009. DOI 10.1016/B978-1-85617-557-9.X0001-2.

White, F., “Fluid Mechanics”, 4th Edition, 1997.

Calçada, L. A., Eler, F. M., Paraiso, E. C. H, Scheid, C. M., Rocha, D. C, “Pressure drop in tool joints for the flow of water-based muds in oil well drilling” Brazilian Journal of Petroleum and Gas V.6 n.4, p. 145-157, 2012. DOI: 10.5419/bjpg2012-0012

Jeong, Y., Shah, S. N., “Analysis of toll joint effects for accurate friction pressure loss calculations”, IADC/SPE 87182, Drilling Conference, Dallas, TX, 2004.

Souza Mendes, P. R., Naccache, M. F., Vargas, P. R., Marchesini, F. H. “Flow of viscoplastic liquids through axisymmetric expansions–contractions”, J. Non-Newtonian Fluid Mech, 2006. doi:10.1016/j.jnnfm.2006.09.00

7. RESPONSIBILITY NOTICE

The authors are the only responsible for the printed material included in this paper.